International Journal of Computer Information Systems and Industrial Management Applications
ISSN 2150-7988 Volume 18 (2026) pp. 1-14

https://doi.org/10.70917/ijcisim-2026-0157
Article

Intelligent Algorithm-Based Multiple Logic Transmission Paths for Common Wealth in Ideological and Political Courses in Colleges and Universities

Shujun Zhang *

School of Marxism, Wuhan Qingchuan University, Wuhan, Hubei, 430204, China; zhangshujun1986@126.com

Abstract: This study utilizes panel data from 30 provinces (regions and municipalities) spanning the years 2015–2024 and employs dynamic QCA methods to identify the dissemination pathways for promoting common prosperity in higher education ideological and political courses. To validate the reliability of this dissemination pathway, a parameter inversion method based on neural networks was designed. First, a modified SIR epidemic model was selected to construct a common prosperity dissemination model. Then, MATLAB R2014 was used to perform parameter inversion for the dissemination model. Finally, model fitting and trend prediction analysis were conducted for the dissemination of common prosperity. Taking institutional development data as an example, the more dispersed the distribution of institutional development values, the fewer citizens holding extreme opinions during the early stages of common prosperity, and the more stable the dissemination of common prosperity. Validating the extracted real-world data, the model established in this study aligns with the actual trend changes, providing valuable insights for researching the dissemination trends of common prosperity.

Keywords: dynamic QCA; SIR; parameter inversion; common prosperity

1. Introduction

With the continuous development of artificial intelligence technology, intelligent algorithms are increasingly being applied to the field of education [1]. Ideological and political education is an important means of cultivating qualified citizens, and the effective communication of ideological and political education content is of great significance for the comprehensive development of students [2-3]. Traditional ideological and political education methods face various challenges, such as simple content, weak interactivity, and lack of targeting [4]. With the rapid development of intelligent algorithms and other artificial intelligence technologies, their application in the dissemination of ideological and political education content offers a new approach to addressing these challenges [5-6]. Under smart education, the delivery of ideological and political education content must possess strong timeliness and appeal, provide students with personalized learning paths, evoke emotional resonance among students, stimulate their interest in learning, and encourage active thinking and in-depth exploration [7-8].

The application of intelligent algorithms in online ideological and political education in higher education institutions primarily achieves personalized content delivery and learning effectiveness assessment through data mining, machine learning, and artificial intelligence technologies. Huang et al. [9] developed a personalized educational resource recommendation user model and improved the collaborative filtering algorithm, enabling personalized recommendations for ideological and political education textbooks, providing students with digital learning channels and enhancing their interest in ideological and political education. Hu [10] proposed a method to integrate artificial intelligence and cloud computing technology (AIIOE) into online English teaching for ideological and political courses in higher education institutions. This method utilizes natural language processing, machine learning, and

cloud computing technology to provide students with personalized and interactive learning experiences. The results showed that under the AIIOE model, students' English proficiency, knowledge of ideological and political issues, and overall learning experience significantly improved.

The rise of new media and the application of intelligent algorithms have driven the efficient integration and sharing of ideological and political education resources, overcoming the limitations of traditional teaching resource distribution [11]. Yun et al. [12] applied deep learning radial basis function neural networks to an innovative ideological and political education platform. Evaluation results of teaching quality showed an average percentage error rate of 88.87%, a reduction in political risk rate during teaching of 83.86%, the student evaluation rate was 76.80%, the predicted teaching error rate was 79.13%, and the overall teaching quality performance was 86.55%. Additionally, regarding research on the dissemination of ideological and political education, Li [13] proposed a conversion algorithm to enhance the effectiveness of dissemination pathways, applying particle information search technology to ideological and political education dissemination. Analysis of experimental results indicates that the proposed model effectively improves the teaching efficiency of ideological and political education.

With the rapid development of information technology today, traditional methods of ideological and political education have faced significant challenges. Therefore, how to effectively utilize modern information technology, especially intelligent algorithms, to improve the efficiency and effectiveness of ideological and political education content delivery has become an important task in the current reform and development of ideological and political education [14].

Firstly, using the dynamic QCA method, the communication paths to promote common prosperity are extracted into four paths: "system-technology" linkage, "resource endowment, large-scale system construction", "resource endowment, system construction, technological innovation" and "public service". Then, a SIR infectious disease model was established to show the number of people concerned about common prosperity and its daily changes. Then, the Runge-Kutta method is used to effectively predict the development trend of the number of followers in the next few days under the condition of different parameter values, and finally the parameters are inverted by the BP neural network algorithm, which effectively fits the network communication trend of common prosperity in the ideological and political courses of colleges and universities.

2. Research on the Multiple Logical Communication Pathways of Common Prosperity

2.1. Research Methods

2.1.1. Method Selection

This paper uses the QCA method to explore the causal complexity of common prosperity levels in ideological and political courses in colleges and universities. Qualitative comparative analysis (QCA) transcends the traditional boundaries between qualitative and quantitative methods [15]. The sample of provinces in China is medium-sized, and the data scale is compatible with this research method.

2.1.2. Samples and Data

This study uses 30 provinces (cities) and autonomous regions in mainland China as its sample (Tibet data is missing), and constructs a common prosperity evaluation indicator system based on five dimensions: resource endowment, institutional development, technological innovation, scale, and public services. Fifteen secondary indicators were selected to form this system. Panel data from 2015 to 2024 were selected as the research object. The relevant data were obtained from the China Statistical Yearbook and the National Bureau of Statistics website. The relevant indicators are shown in Table 1.

Table 1. Common prosperity evaluation index system.

Primary indicator	Secondary indicator
Endowment of resources	Land efficiency
	Capital investment
	Labor utilization level
Institutional construction	Profitability
	Managerial ability

	Supervisory ability
Technical innovation	Technical output level
	Financial input level
	R&D input level
Scale	Land scale
	Technology scale
	Service scale
Public service	Education service level
	Health care level
	Level of public infrastructure construction

2.1.3 Measurement and calibration

In QCA analysis, each condition variable and outcome variable can be regarded as an independent set, and each case has membership scores across multiple sets. First, based on the actual development conditions of each province, the value distributions of the variables are determined, and then the three "anchor points" of "complete membership," "crosspoint," and "complete non-membership" are established. The three calibration points for each variable are set as the 95th, 50th, and 5th percentiles of the sample data, respectively. The calibration results are shown in Table 2.

Table 2. Calibration results.

Variable classification	Variable name	Full membership	Crossing point	Completely unaffiliated
Result variable	Common prosperity (Y)	0.564	0.309	0.181
Conditional variable	Endowment of resources (X1)	0.07	0.038	0.027
	Institutional construction (X2)	0.067	0.027	0.009
	Technical innovation (X3)	0.132	0.03	0.005
	Scale (X4)	0.098	0.042	0.0011
	Public service (X5)	0.056	0.017	0.018

2.2. Results and Analysis

2.2.1. Analysis of the necessity of individual conditions

Dynamic QCA and traditional QCA are similar in their necessity testing steps, both using consistency level and coverage as two indicators to measure necessary conditions. When the consistency level of a condition variable exceeds 0.9 and the coverage exceeds 0.5, that condition can be considered a necessary condition for the outcome variable. Additionally, when the adjustment distance is less than 0.2, it indicates a high level of aggregated consistency precision, providing stronger support for the judgment of the results. For causal combinations where the adjustment distance exceeds 0.2, further analysis of intergroup consistency, intergroup coverage, and X-Y scatter plots is required.

As shown in Table 3, it can be seen that for both high-level common prosperity and low-level common prosperity, the summary consistency of the five variables—resource endowment, institutional development, technological innovation, scale, and public services—is below 0.9, indicating that these five antecedent conditions are not necessary conditions for the outcome variable, and the explanatory power of individual conditions is weak.

Table 3. Analysis of necessary conditions.

Conditional variable	High levels of common prosperity (Y)				Low levels of common prosperity (Y^*)			
	Aggregate consistency	Aggregate coverage	Intergroup consistency alignment distance	Within group consistency alignment distance	Aggregate consistency	Aggregate coverage	Intergroup consistency alignment distance	Within group consistency alignment distance
X1	0.763	0.734	0.037	0.326	0.567	0.636	0.29	0.409
~X1	0.636	0.567	0.119	0.356	0.777	0.759	0.084	0.282
X2	0.832	0.745	0.268	0.17	0.448	0.495	0.717	0.438
~X2	0.425	0.42	0.642	0.344	0.758	0.842	0.587	0.132
X3	0.79	0.882	0.075	0.412	0.448	0.562	0.331	0.597
~X3	0.596	0.489	0.088	0.437	0.874	0.829	0.046	0.198
X4	0.687	0.734	0.039	0.443	0.561	0.647	0.24	0.544
~X4	0.645	0.558	0.155	0.42	0.765	0.741	0.061	0.321
X5	0.665	0.622	0.095	0.462	0.636	0.718	0.123	0.387
~X5	0.707	0.632	0.124	0.429	0.663	0.66	0.25	0.411

Additionally, further analysis was conducted on cases where the intergroup consistency adjustment distance exceeded 0.2 in Table 3, with the specific results shown in Table 4. First, the intergroup consistency and intergroup coverage of Cases 1, 3, 4, 6, and 7 all failed to meet the evaluation criteria, so these combinations do not exhibit a necessary relationship. Second, in Scenario 2, the consistency exceeded 0.9 and the coverage exceeded 0.5 during the 2021–2024 period. The X-Y scatter plot is shown in Figure 1, with (a) and (b) representing the sample scatter plots for 2021 and 2024, respectively. By comparing the X-Y scatter plots, it was found that the distribution of sample points does not meet the requirements. Therefore, during the 2021–2024 period, this condition variable did not pass the necessary condition test. Similarly, Situation 5 also failed the necessity test during the 2015–2019 period. Finally, based on the intergroup consistency trends in Scenarios 1, 3, 6, and 7 in Table 4, it can be observed that as the rural revitalization strategy progresses, the roles of resource endowments, institutional development, technological innovation, and scale expansion in promoting common prosperity are showing an upward trend.

Table 4. The consistency of the group is more than 0.2.

Case	Causal combination	Index	2015	2016	2017	2018	2019	2020	2021	2022	2023	2024
1	X1-Y*	Intergroup consistency	0.434	0.486	0.416	0.468	0.594	0.591	0.727	0.736	0.816	0.869
		Intergroup coverage	0.855	0.834	0.732	0.702	0.703	0.623	0.58	0.603	0.516	0.431
2	X2-Y	Intergroup consistency	0.629	0.652	0.625	0.609	0.589	0.725	0.922	0.982	0.985	0.985
		Intergroup coverage	0.723	0.814	0.857	0.892	0.937	0.872	0.727	0.658	0.683	0.766

3	X2-Y*	Intergroup consistency	0.208	0.2	0.222	0.235	0.311	0.559	0.851	0.986	0.992	1
		Intergroup coverage	0.772	0.664	0.608	0.648	0.584	0.613	0.508	0.436	0.352	0.28
4	X*2-Y	Intergroup consistency	0.821	0.729	0.726	0.751	0.74	0.691	0.411	0.125	0.094	0.106
		Intergroup coverage	0.232	0.268	0.314	0.365	0.477	0.61	0.761	0.937	1	0.994
5	X*2-Y*	Intergroup consistency	0.937	0.918	0.964	0.978	0.961	0.878	0.57	0.198	0.13	0.19
		Intergroup coverage	0.884	0.885	0.849	0.824	0.719	0.757	0.866	0.938	0.934	0.931
6	X3-Y*	Intergroup consistency	0.325	0.349	0.358	0.365	0.453	0.519	0.564	0.635	0.692	0.721
		Intergroup coverage	0.716	0.713	0.652	0.641	0.601	0.571	0.54	0.51	0.442	0.381
7	X4-Y	Intergroup consistency	0.429	0.444	0.511	0.481	0.565	0.605	0.61	0.655	0.766	0.799
		Intergroup coverage	0.85	0.821	0.791	0.755	0.71	0.646	0.579	0.534	0.508	0.393
8	X5-Y*	Intergroup consistency	0.647	0.621	0.6	0.515	0.552	0.59	0.66	0.833	0.937	0.967
		Intergroup coverage	0.888	0.826	0.765	0.741	0.658	0.638	0.625	0.612	0.542	0.413

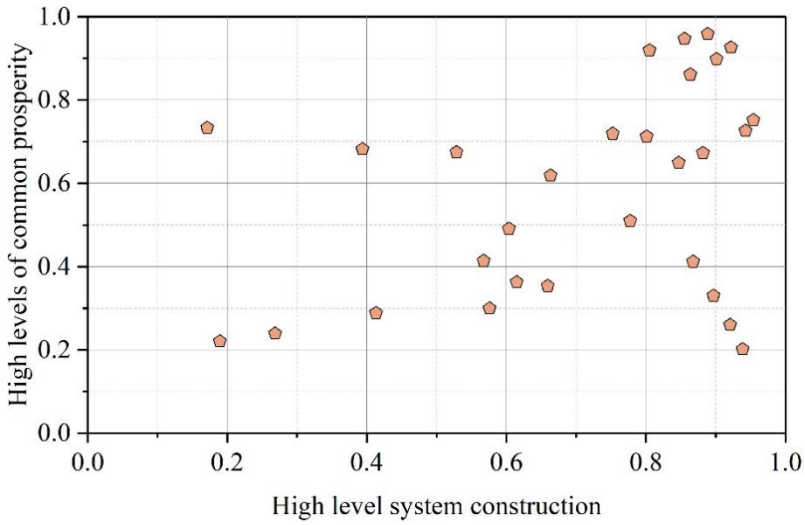

(a) Sample scatter diagram in 2021

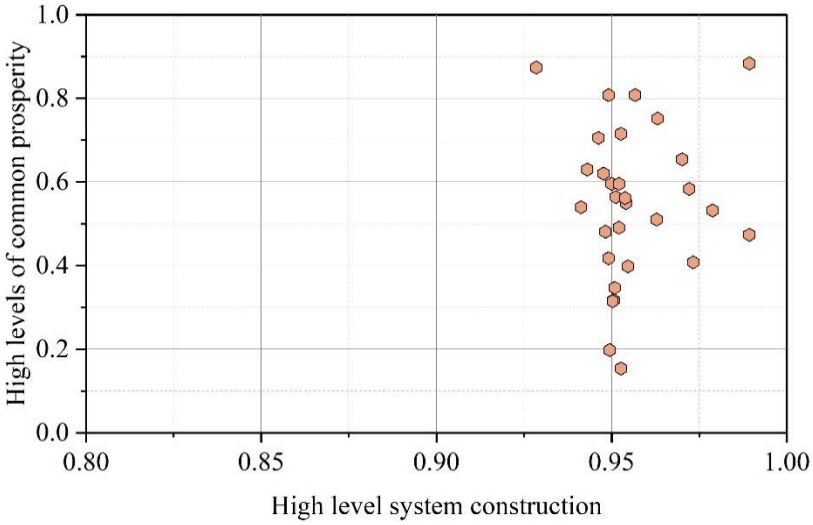

(b) Sample scatter diagram in 2024

Figure 1. Scatter diagram group diagram.

2.2.2. Analysis of the adequacy of condition configuration

The core of dynamic QCA lies in analyzing the impact of different condition combinations on the outcome variable, with consistency levels serving as an important evaluation criterion. Based on existing research, the consistency threshold is generally set at 0.75 or higher. Referring to relevant literature and the sample conditions of this paper, the original consistency threshold is set to 0.8, the frequency threshold to 1, and the PRI threshold (inverse inconsistency ratio threshold) to 0.6, to construct the truth table. The analysis results are shown in Table 5. This paper identifies two configuration paths for high-level common prosperity and five configuration paths for low-level common prosperity. The overall consistency for high- and low-level common prosperity is 0.905 and 0.897, respectively, both exceeding 0.75. The overall coverage and consistency of each configuration also meet the evaluation criteria. Additionally, the inter-group consistency adjustment distance and intra-group consistency adjustment distance are both below 0.2, demonstrating strong explanatory power. By summarizing the configurations for high- and low-level common prosperity, four transmission pathways influencing the level of common prosperity were identified: the "institutional-technological" linkage type, with configuration a1; the "resource endowment + institutional development + scale" driven type, with configuration a2; the "resource endowment + institutional development + technological innovation" constrained type, with configuration b3; and the "public services" constrained type, which encompasses configurations b4 and b5.

Table 5. Results of common prosperity configuration analysis.

Conditional variable	Configuration analysis - high		Configuration analysis - low				
	a1	a2	b1	b2	b3	b4	b5
Consistency	0.939	0.942	0.959	0.986	0.991	0.915	0.986
PRI	0.876	0.843	0.891	0.918	0.969	0.694	0.892
Coverage	0.668	0.398	0.481	0.45	0.573	0.294	0.253
Unique coverage	0.358	0.087	0.074	0.121	0.122	0.025	0.008
Intergroup consistency alignment distance	0.034	0.089	0.03	0.075	0.056	0.088	0.019
Within group consistency alignment distance	0.1	0.115	0.083	0.098	0.106	0.12	0.142
Overall consistency	0.905		0.897				

General PRI	0.865	0.839
Overall coverage	0.733	0.791

3. Predicting the dissemination pathways of multiple logics of common prosperity in ideological and political courses

This chapter constructs a common prosperity propagation model using the SIR infectious disease model. Subsequently, the Runge-Kutta method and BP neural network technology are employed in conjunction with actual propagation data to invert model parameters. Taking "institutional development" as an example, the model is fitted and trend predictions are analyzed.

3.1. Research Methods

3.1.1. Revision of the SIR infectious disease model

Symbolic assumptions: $S(t)$ denotes the number of susceptible individuals, $I(t)$ denotes the number of infected individuals, $R(t)$ denotes the number of removed individuals (with antibodies), $D(t)$ denotes the number of deceased individuals, β denotes the transmission rate (effective transmission rate per individual per unit time), and γ denotes the removal rate. $\gamma = \gamma_1 + \gamma_2$, where γ_1 denotes the recovery rate (the rate of recovery per unit time), and γ_2 denotes the mortality rate (the rate of death per unit time) [16].

Assuming that the natural birth rate is equal to the natural death rate, the modified SIR model is:

$$\frac{dS(t)}{dt} = -\beta I(t)S(t), t > 0 \tag{1}$$

$$\frac{dI(t)}{dt} = \beta I(t)S(t) - \gamma I(t), t > 0 \tag{2}$$

$$\frac{dR(t)}{dt} = \gamma_1 I(t), t > 0 \tag{3}$$

$$\frac{dD(t)}{dt} = \gamma_2 I(t), t > 0 \tag{4}$$

The initial conditions correspond to:

$$S(0) = S_0, I(0) = I_0, R(0) = 0, D(0) = 0 \tag{5}$$

From the assumption, it can be seen that the total population $N = S(t) + I(t) + R(t) + D(t) = S_0 + I_0$ is a constant.

If the parameters γ_1, γ_2, and β in the modified SIR model and the initial conditions are all known, then problems (1) to (5) are called the direct problems of the modified SIR model. Below, we derive the expressions for the solutions to the direct problems.

From equations (1) and (3), we obtain: $\frac{\mathrm{d}S(t)}{\mathrm{d}R} = -\frac{\beta}{\gamma_1}S(t)$. By separating variables, we obtain $S(t) = C_1 e^{-\frac{\beta}{\gamma_1}R(t)}$. From $S(0) = S_0$ and $R(0) = 0$, we obtain $S_0 = C_1 e^0$, hence:

$$S(t) = S_0 e^{-\frac{\beta}{\gamma_1}R(t)} \tag{6}$$

Let N be a constant, then $I(t) = N - S(t) - R(t) - D(t)$, i.e., $I(t) = N - S_0 e^{-\frac{\beta}{\gamma_1}R(t)} - R(t) - D(t)$.

From equation (3) and the initial conditions, we obtain:

$$\begin{cases} \dfrac{dR(t)}{dt} = \gamma_1 \left(N - S_0 e^{-\frac{\beta}{\gamma_1} R(t)} - R(t) - D(t) \right) \\ R(0) = 0 \end{cases} \tag{7}$$

From equations (3) and (4), we can see that $\dfrac{dR(t)}{dD} = \dfrac{\gamma_1}{\gamma_2}$, so we have $R(t) = \dfrac{\gamma_1}{\gamma_2} D(t) + C_2$. From $R(0) = D(0) = 0$, we get $C_2 = 0$, that is:

$$D(t) = \frac{\gamma_2}{\gamma_1} R(t) \tag{8}$$

From equations (7) and (8), we obtain:

$$\frac{dR(t)}{dt} = \gamma_1 \left(N - S_0 e^{-\frac{\beta}{\gamma_1} R(t)} - R(t) - \frac{\gamma_2}{\gamma_1} R(t) \right) \tag{9}$$

Thus, the patterns of changes in the number of susceptible individuals, infected individuals, individuals with antibodies, and deceased individuals are obtained as the following coupled system of explicit equations (including explicit differential equations, explicit transcendental equations, and explicit algebraic equations):

$$\begin{cases} \dfrac{dR(t)}{dt} = \gamma_1 \left(N - S_0 e^{-\frac{\beta}{\gamma_1} R(t)} - R(t) - \dfrac{\gamma_2}{\gamma_1} R(t) \right), t > 0 \\ S(t) = S_0 e^{-\frac{\beta}{\gamma_1} R(t)}, t > 0 \\ D(t) = \dfrac{\gamma_2}{\gamma_1} R(t), t > 0 \\ I(t) = N - S_0 e^{-\frac{\beta}{\gamma_1} R(t)} - R(t) - D(t), t > 0 \\ S(0) = S_0, I(0) = I_0, R(0) = 0, D(0) = 0 \end{cases} \tag{10}$$

From the analysis of the above decoupled equation system, it can be seen that if the analytical solution of $R(t)$ can be obtained, then the solutions of $S(t)$, $D(t)$, $I(t)$ can be derived. Unfortunately, the analytical solution of the initial value problem (7) is difficult to obtain and requires numerical computation. From the form of the decoupling equations, the key is to compute the numerical solution of the initial value problem (7). Clearly, $f(R) = \gamma_1 \left(N - S_0 e^{-\frac{\beta}{\gamma_1} R(t)} - R(t) - \dfrac{\gamma_2}{\gamma_1} R(t) \right)$ is differentiable with respect to R. Therefore, the right-hand side $f(R)$ of the differential equation corresponding to the initial value problem (7) is Lipschitz continuous with respect to R and Lipschitz bounded. By the existence and uniqueness theorem for ordinary differential equations, the initial value problem (8) has a unique solution, so a numerical algorithm can be designed to find the numerical solution to this initial value problem.

3.1.2. Runge-Kutta method

The Runge-Kutta method is a class of implicit or explicit iterative methods used to solve systems of nonlinear ordinary differential equations. It is widely applied in engineering fields, characterized by high accuracy but also a relatively complex implementation principle [17].

Among various Runge-Kutta methods, the most commonly used is the classical fourth-order method, also known as "RK4." This method uses computer simulation technology to replace the complex solution process of higher-order differential equations when the derivatives and initial values of the equations are known.

For example, let the initial value problem be expressed as follows:

$$\begin{cases} \dfrac{dy}{dt} = f(t, y) \\ y(t_0) = y_0 \end{cases} \tag{11}$$

Then, solving this problem using the fourth-order Runge-Kutta method can be expressed as:

$$y_{n+1} = y_n + \frac{h}{6}(k_1 + 2k_2 + 2k_3 + k_4) \tag{12}$$

Among them:

$$\begin{cases} k_1 = f(t_n, y_n) \\ k_2 = f\left(t_n + \dfrac{h}{2}, y_n + \dfrac{h}{2}k_1\right) \\ k_3 = f\left(t_n + \dfrac{h}{2}, y_n + \dfrac{h}{2}k_2\right) \\ k_4 = f(t_n + h, y_n + hk_3) \end{cases} \tag{13}$$

From the above formula, it can be seen that the value of (y_{n+1}) depends on the sum of the current value (y_n) plus the time interval (h) multiplied by a slope, where k_1, k_2, k_3, k_4 represent the slopes at the beginning, midpoint, and end of each time interval, respectively. The value of y for each time interval is determined by the slope of the previous time interval.

3.1.3. BP Neural Network

BP neural networks use the backpropagation algorithm to continuously adjust the thresholds and parameter weights in the network until the overall network error is minimized, thereby achieving the desired output. Also known as feedforward neural network models, their network model topology mainly consists of three layers: the input layer, the hidden layer, and the output layer. The hidden layer in the middle can be a single layer or composed of multiple layers [18], as shown in Figure 2.

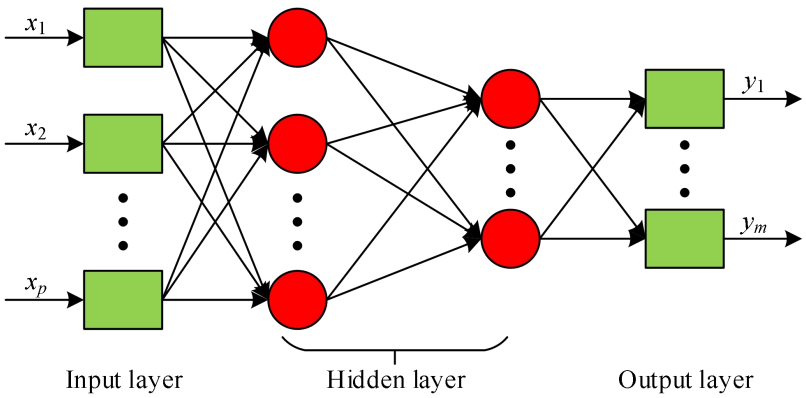

Figure 2. BP Neural topology.

The input signal to the network is processed by the input layer and hidden layer special functions, and then reaches the output layer. The output results of the neural network are compared with the expected results of the samples. If the error between the two is significant, the error backpropagation process is initiated. In this process, the error signal propagates backward through the output layer, hidden layer, and input layer, distributing the error to the neurons in each layer. This process modifies and optimizes the weights and thresholds of the entire network, gradually bringing the actual output values of the neural network closer to the expected output values until the network converges. To implement error feedback in a BP neural network, an error function must first be defined. Assume that the neural network has p

samples to be learned, denoted as $x^1, x^2, \cdots, x^p$, and the actual output obtained after inputting these samples into the network is $y_j^p \left(j = 1, 2, \cdots, m \right)$. If the objective function value of the neural network is set as a squared error function, then E_p represents the error of the p th learning sample:

$$E_p = \frac{1}{2} \sum_{j=1}^{m} \left(t_j^p - y_j^p \right)^2 \tag{14}$$

Among them, t_j^p —expected output.

The global error calculation formula for the learning sample is:

$$E = \frac{1}{2} \sum_{p=1}^{p} \sum_{j=1}^{m} \left(t_j^p - y_j^p \right)^2 = \sum_{p=1}^{p} E_p \tag{15}$$

The global error E of the BP neural network is mainly used to repeatedly train and optimize the network weights so that the error of the network output meets the error accuracy. Generally, a specified learning rate is used to optimize the network weights. Assuming that the above calculation method is used to determine the global error, and based on this, the connection weight coefficient ω_{jk} is adjusted by introducing the learning rate η so that:

$$\Delta \omega_{jk} = -\eta \frac{\partial E}{\partial \omega_{jk}} = -\eta \frac{\partial}{\partial \omega_{jk}} \left(\sum_{p=1}^{p} E_p \right) = \sum_{p=1}^{p} \left(-\eta \frac{\partial E}{\partial \omega_{jk}} \right) \tag{16}$$

BP neural networks can self-learn and adaptively process data, enabling them to accurately approximate complex nonlinear relationships. The dissemination of common prosperity is a complex, dynamic, nonlinear process that changes over time. Based on the patterns and characteristics of common prosperity development, BP neural network technology can be used to predict its dissemination trends.

3.1.4. Parameter inversion algorithm

After determining the SIR model for the spread of common prosperity, the system of ordinary differential equations for the model is obtained. The Runge-Kutta method is used to solve the system of ordinary differential equations for the SIR model, yielding numerical solutions for $I(t)$ and $In(t)$. Different parameter values correspond to distinct sets of numerical solutions. Then, using BP neural network technology, the numerical solutions of the model are used as input values for the neural network, and the corresponding parameter values are used as network outputs to construct the training samples for the neural network. Based on this, a nonlinear mapping relationship between the numerical solutions of the model and the model parameter values is established. Using MATLAB software to train the neural network, real common prosperity propagation data is then used as input values to perform parameter inversion for the common prosperity propagation model. Finally, the model parameter values obtained from the inversion can be used to predict the propagation trend of common prosperity.

The steps of the parameter inversion algorithm are designed as follows:

(1) Determine the value range G_A of the parameter set $A(\alpha, \beta, \gamma, \lambda, \mu)$ in the SIR transmission model, and randomly select N sets of parameter values $A_i \left(a_i, \beta_i, \gamma_i, \lambda_i, \mu_i \right)$, where $A_i \in G_A$ and $i = 1, 2, \ldots, n$.

(2) For each set of parameter values A_i, given the initial value S_0, I_0, In_0, R_0, use the Runge-Kutta method to solve the ordinary differential equation system (10), and use the numerical solutions $I_{i1}, I_{i2}, \ldots I_{iM}$ and $In_{i1}, In_{i2}, \ldots, In_{iM}$ obtained for groups $I(t)$ and $In(t)$ of N as the input values of the network. The output values of the network are the parameter values A_i corresponding to the numerical solutions, which are used to construct the training samples and test samples.

(3) Train the neural network.

(4) Use the actual common prosperity propagation data $I(1), I(2), \ldots, I(M), In(1), In(2), \ldots, In(M)$ as the input values for the neural network to obtain the parameter set A of the SIR model through inversion.

3.2. Analysis of Simulation Results

To validate the reasonableness and feasibility of the model, this paper uses Matlab software to construct a BA scale-free network. To ensure that the simulation closely resembles the evolution process of real-world network public opinion, nodes in the network are sorted from largest to smallest based on their degree, and the top 20 nodes are selected as initial infected nodes for simulation and modeling. The previous section identified four transmission pathways influencing the level of common prosperity using the QCA method, among which institutional development has the greatest impact on transmission pathways. Therefore, this section conducts a detailed analysis and validation of the model based on institutional development factors.

Nodes with institutional development values following random and normal distributions exhibit different evolution processes for infected and recovered individuals, as shown in Figure 3. (a) and (b) represent the changes in the density of infected and recovered individuals under different distribution rules of institutional development values. When institutional development values follow a normal distribution, the rate of increase and peak of the infected population density curve are higher than those of the infected population density curve when institutional development values follow a random distribution. Similarly, the rate of increase and peak of the recovered population density curve are also higher than those of the recovered population density curve when institutional development values follow a random distribution. Through analysis of the simulation results, combined with the common prosperity propagation model in this paper, the following conclusions can be drawn: When the institutional construction value distribution follows a normal distribution, it means that in the early stages of common prosperity, some members of the public have strong opinions and extremely similar views, and the public's opinions will have a certain degree of homogeneity in the early stages. Therefore, under the same opinion threshold, more members of the public will accept information similar to their own opinions, meaning that more susceptible individuals will become propagators.

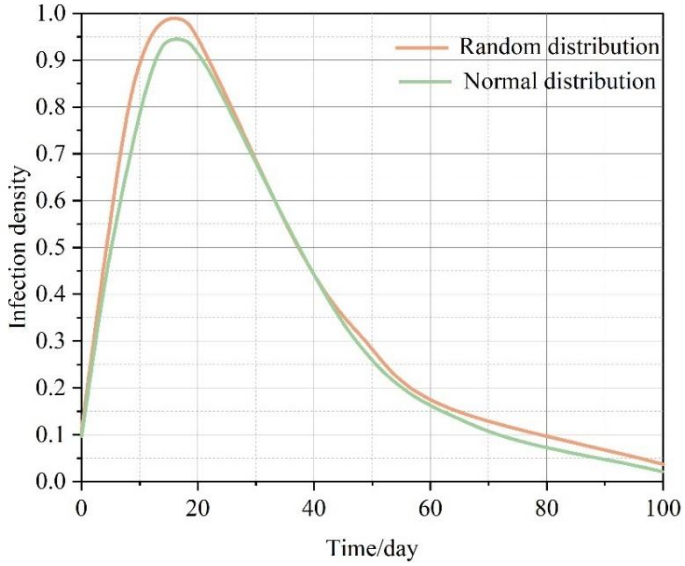

(a) Change in the density of infected people

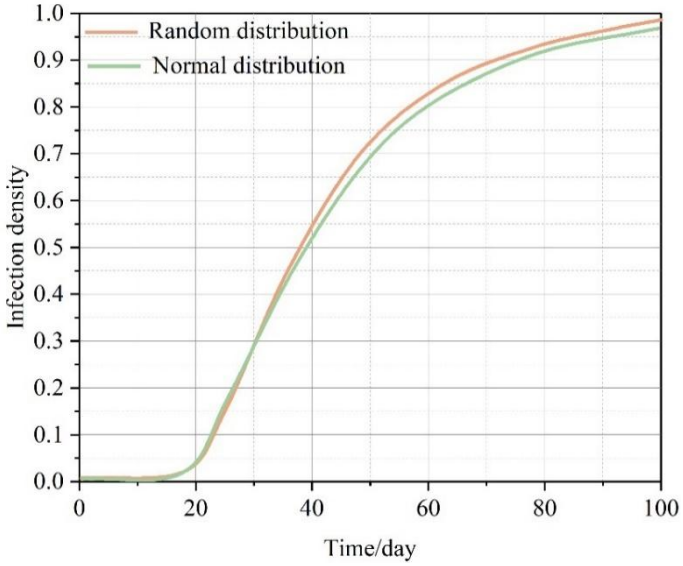

(b) Comer density variation

Figure 3. System construction affects the transmission process.

3.3. Case Study

3.3.1. Data Acquisition

By analyzing institutional construction data obtained through web crawling, the relationship between time and the number of infected individuals is shown in Figure 4. The graph of time and the number of infected individuals exhibits a segmented pattern. The graph shows three distinct phases of growth and decline, with the peaks of each segment decreasing over time. The first phase spans from Day 1 to Day 7. The second phase spans from Day 8 to Day 18. The third phase spans from Day 19 to Day 25.

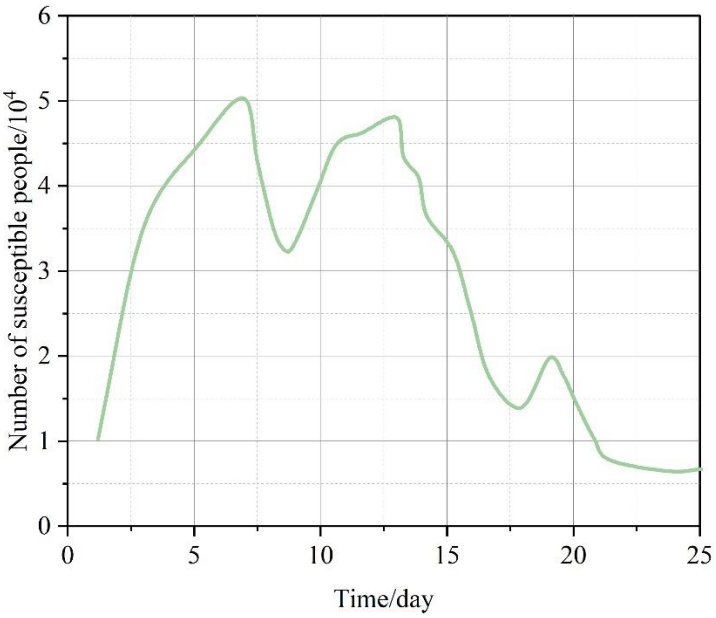

Figure 4. Time and number of people infected.

3.3.2. Solution Process and Result Analysis

The parameter ranges for the SIR model are selected as follows: $\alpha \in [0.00002, 0.00002]$, $\beta \in [0.3112, 0.4002]$, $\gamma \in [0.02, 0.03]$, $\lambda \in [0.003, 0.015]$, $\mu \in [0.022, 0.033]$. Within the above parameter ranges, 3000 sets of parameters were selected using a fixed step size. The numerical

solution of $I(t)$ was determined using the Runge-Kutta method and used as the input to the BP neural network. with its original parameters as the output values of the neural network. The number of nodes in the input layer, hidden layer, and output layer of the network are set to 6, 5, and 5, respectively, with a learning rate of 0.05, target error of 0.01, training algorithm trainbr, transfer function tansig, and maximum iteration count of 1000. Based on the above training samples, the neural network is trained until the error criteria are met.

Once the network is trained, the data from the 10 days prior to the event is used as input values to invert and determine the parameter values of the SIR model. To minimize the impact of errors, this process is repeated 100 times, and the average value of the parameters $A(\alpha, \beta, \gamma, \lambda, \mu)$ is calculated. This average value is then substituted into the SIR model to predict the trend of the "common prosperity" network's spread.

The trend of time and the number of infected individuals is shown in Figure 5. The parameter inversion method accurately predicted the trend of time and the number of infected individuals in the first segment of change. From day 1 to day 4, the number of infected individuals was relatively close, and the peak occurrence time of the actual data and the predicted data was the same, which was day 7. The trend of the predicted common prosperity spread data based on the parameter inversion algorithm is basically consistent with the actual spread data, and the error is also small. This indicates that the parameter inversion algorithm based on neural network technology can be used to simulate the spread process of common prosperity and predict its spread trend based on the SIR model of common prosperity spread constructed in this paper.

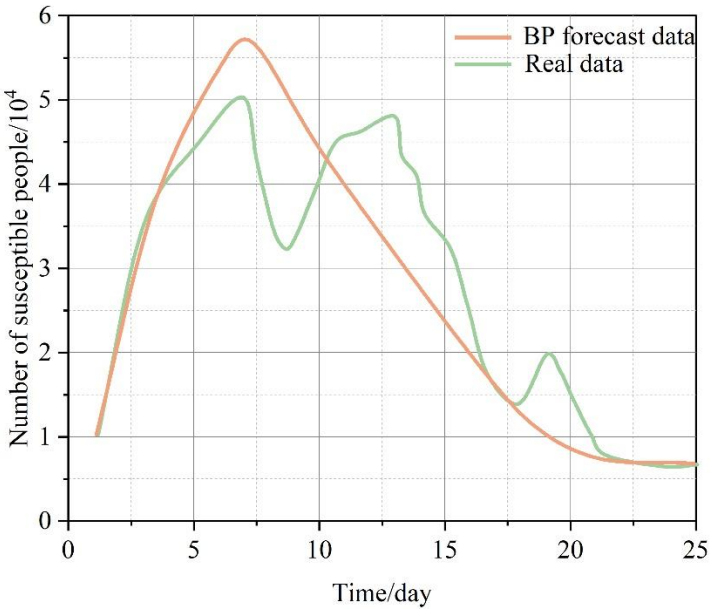

Figure 5. Time and number of people infected.

The study utilizes panel data from 30 provinces (regions and municipalities) spanning the years 2015–2024 and employs dynamic QCA methods to explore the configuration pathways that drive improvements in common prosperity levels. The findings indicate that in the process of empowering common prosperity, common prosperity levels are influenced by multiple factors, and no single factor can independently drive its improvement. Both high and low levels of common prosperity exhibit seven configuration paths, among which four are identified: the "institutional-technological" linkage type, the "resource endowment + institutional development + scale" driven type, the "resource endowment + institutional development + technological innovation" constrained type, and the "public services" constrained type.

To validate the reliability of the dissemination pathways, a model fitting and trend prediction analysis was conducted using "institutional development" as an example. The model fitting values showed minimal deviation from actual values, indicating that the parameter inversion method based on neural networks designed in this study can effectively predict the dissemination pathways of common prosperity in higher education ideological and political courses.

Funding
This research was supported by the Educational Science Planning Project of Hubei Provincial Department of Education in 2019. Project Name: "Research on the Characteristics of Ideological and Political Work of Private Colleges and Universities and the Innovation of Educational Mechanism" (Project No: 2019GB102).

References

1. Luan, H., Geczy, P., Lai, H., Gobert, J., Yang, S. J., Ogata, H., ... & Tsai, C. C. (2020). Challenges and future directions of big data and artificial intelligence in education. Frontiers in psychology, 11, 580820.
2. Li, L. (2017). Teaching of ideological and political education for college students from the perspective of culture. DEStech Transactions on Social Science Education and Human Science, 1, 656-661.
3. Lingli, Y. (2021). A Study on the Cultivation Path of Patriotic Feelings in the Ideological and Political Education of College Students. Journal of Frontiers in Educational Research, 1(4), 74-77.
4. Qing, Z. (2024). Innovating Content and Methods of Ideological and Political Education in the Context of the New Era. International Journal of Education and Humanities, 4(4), 479-487.
5. Xu, C., & Wu, L. (2024). The Application of Artificial Intelligence Technology in Ideological and Political Education. International Journal of Advanced Computer Science & Applications, 15(1).
6. Jianzhan, W., & Chennuo, X. (2024). The Theory and Path of Ideological and Political Course Construction in the Era of Artificial Intelligence. Frontiers in Educational Research, 7(8).
7. Zixuan, P. (2022). Literature Review on Intelligent Media of Ideological and Political Education. Academic Journal of Humanities & Social Sciences, 5(5), 10-17.
8. Liu, W., & He, C. (2022). Curriculum-Based Ideological and Political Education: Research Focuses and Evolution. International Education Studies, 15(5), 28-35.
9. Huang, P. (2024). Research on Personalized Ideological and Political Education Content Distribution System Based on Intelligent Algorithms. International Journal of High Speed Electronics and Systems, 2540151.
10. Hu, W. (2023). A new artificial intelligence based internet online English teaching model with curriculum of ideological and political concern. International Journal on Recent and Innovation Trends in Computing and Communication, 11(6s), 177-186.
11. Zhang, K. (2024). Design and application of intelligent teaching system for network and new media major driven by artificial intelligence technology. International Journal of Embedded Systems, 17(1-2), 150-159.
12. Yun, G., Ravi, R. V., & Jumani, A. K. (2023). Analysis of the teaching quality on deep learning-based innovative ideological political education platform. Progress in Artificial Intelligence, 12(2), 175-186.
13. Li, L. (2023). Effective model of the communication path conversion of ideological and political education in colleges and universities based on new media. Computer-Aided Design and Applications.
14. Yu, H. (2022). Intelligent Algorithm to Push the Platform Design of University Management System. In Innovative Computing: Proceedings of the 4th International Conference on Innovative Computing (IC 2021) (pp. 1609-1613). Springer Singapore.
15. John Eugene Chrisman. (2024). More frequent and stronger ties? Using QCA to assess the effects of policy in a Norwegian biotech cluster. Regional Studies, Regional Science,11(1),645-659.
16. Liqing Qiu,Wei Jia,Weinan Niu,Mingjv Zhang & Shuqi Liu. (2020). SIR-IM: SIR rumor spreading model with influence mechanism in social networks. Soft Computing,25(22),1-10.
17. Fan Lidan,Zhao Sifan & Han Fengqing. (2021). Research on The Numerical Accuracy of Network Public Opinion Propagation Model Based on Runge-Kutta Method. Journal of Physics: Conference Series,1848(1),
18. Mengyao Xu & Qian Wu. (2020). Analysis of news transmission mode based on fuzzy data classification and neural network simulation. Journal of Intelligent & Fuzzy Systems,38(6),7133-7143.